# A new Volt / var local control strategy in low-voltage grids in the context of the *LINK*-based holistic architecture

**Daniel-Leon SCHULTIS, Albana ILO**

TU Wien – Institute of Energy Systems and Electrical Drives,

Gußhausstraße 25/370-01, 1040 Vienna,

+43 (0)1 58801 370132, daniel-leon.schultis@tuwien.ac.at

**Abstract:**

This paper proposes a new Volt / var control strategy in low-voltage grids in the context of the *LINK*-based holistic architecture. Contrary to the classical approach where customer-owned PV-inverters are used for voltage control, it is proposed to use DSO-owned inductive devices set at the end of the violated low voltage feeders and equipped with *L*(*U*) primary control. This concept is compared to the well-known local *Q*(*U*)-control of PV-inverters. Results show that using Volt / var controls on customer plant side entails social issues in the field of cost allocation, data privacy, and discrimination, and technical issues in the field of cyber security, grid losses, distribution transformer loading and uncontrolled reactive power exchange with the superordinate grid. The use of *L*(*U*)-control mitigates the social issues and shows the best technical behaviour. It simplifies considerably the Volt / var management tasks in low voltage grids.

**Keywords:** Low-voltage grid, Local Volt / var control, Coordinated Volt / var control, Photovoltaic, Inverter, *LINK*-based holistic architecture.

## 1 Introduction

The increasing share of distributed generation (DG) challenges the traditional power system operation. In many cases, they provoke a reverse active power flow that causes violations of the upper voltage limit within the radial structures of the distribution grid [1]. Distribution system operators (DSO), who are obliged to keep the grid voltage within the EN 50160 limits of ±10% around nominal voltage, should take countermeasures to allow the further DG integration. In this regard, Ref. [2] proposes the use of the available DG inverters for voltage control in distribution grids with high DG share. Similar to large power plants that inject reactive power into the transmission grid, DGs should also be included in the voltage control of distribution grid. But, unlike the transmission grid, where the number of connected power plants is small, the number of connected DGs in the low voltage grid (LVG) part of the distribution grids is very large. Additionally, the number of installed rooftop PV-systems increases rapidly [3]. Therefore, DG-owners are required to make the necessary investments in controlling units so that they can connect to the grid. Thus, the costs for LVG voltage control are allocated to the customers.

To alleviate the violation of upper voltage limit, different control strategies are proposed like upgrading the PV-inverters with different local Volt / var control strategies [4,5], sometimes in

combination with active power curtailment [6]. In particular, setting a *Q*(*U*)-characteristic to define the reactive power contribution of PV-inverters is a method that gained much attention in recent years [7]. A *Q*(*U*)-controlled PV-inverter injects or absorbs reactive power depending on the local grid voltage, which varies along the feeder. This control strategy intertwines the operation of LVG with that of the PV-inverters, although they are property of different players. Additionally, it leads to a discriminatory provision of ancillary services. Customers located close to the beginning of the feeder are required to provide less reactive power for LVG voltage control than those located close to its end. This contradicts Ref. [8], where the procurement of non-frequency ancillary services by DSOs is defined as transparent, non-discriminatory and market-based.

Furthermore, the use of local Volt / var control strategies leads to uncontrolled reactive power flows in the superordinate grids making their coordination necessary [9]. The coordination of the reactive power injected by customer-owned PV-inverters requires extensive data exchanges between the DSO and customers [10-12], jeopardizing the strict data privacy and cyber security requirements, and exacerbating the Volt / var management tasks of LVGs. Additionally, local Volt / var controls (e.g. *Q*(*U*)) increase the reactive power flows within LVGs, and thus also grid losses and distribution transformer (DTR) loading [13].

As discussed above, by attempting to reach technical solutions, new social and technical issues are provoked that make the DG implementation in large scale almost impossible. To overcome the actual social and technical problems, this paper proposes a new Volt / var local control strategy, which results from the holistic view of power systems and customer plants [14]. *LINK*-Solution stipulates that each grid operator should primarily use his own reactive devices for voltage control. Therefore, DSO-owned inductive devices are set at the end of the violated feeders and are equipped with local *L*(*U*)-control [13,15,16].

This paper focuses on the analyses of the LVG and medium voltage grid (MVG) behaviour in presence of the uncoordinated local Volt / var controls installed on customer plant or low voltage grid side. Firstly, the rise of the *L*(*U*)-control is described. Secondly, the structures arising from applying *Q*(*U*)- or *L*(*U*)-control for the LVG voltage control are compared. Then, the behaviour of the MVG and LVG in presence of local *Q*(*U*)- and *L*(*U*)-control are separately analysed via load flow simulations. Finally, conclusions are drawn.

# 2 Rise of *L*(*U*)-control

The *L*(*U*)-control in low-voltage grids arises from the *LINK*-based holistic architecture, which stipulates that each grid operator should primarily use his own reactive devices for voltage control.

## 2.1 Holistic view

Figure 1 shows the schematic of the *LINK*-based Volt / var interaction chain. In the European type of distribution grids, DSOs operate the sub-transmission, medium and low voltage grids. The object of this study is the MVG and LVG as conceived in the *LINK*-based holistic architecture [14]. Per definition, each Grid-Link consists of a grid part, called Link_Grid, with the corresponding secondary control and interfaces. Each Link_Grid has a number of Boundary Link Nodes (BLiN) that interconnect adjacent Link_Grids. The facilities within the

Link_Grid, e.g. the transformer and reactive devices, are upgraded with a primary control. They receive set-points from the corresponding Volt / var secondary control (VVSC) which

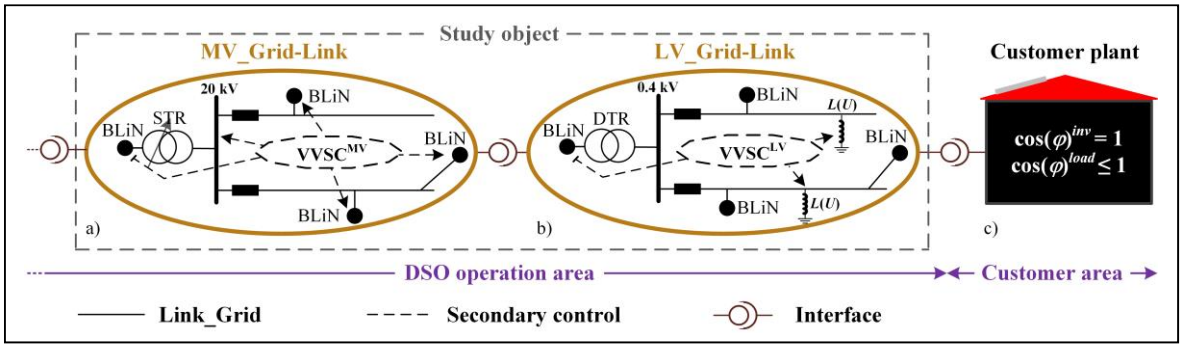


*Figure 1: Schematic of the LINK-based Volt / var interaction chain: a) MV_Grid-Link; b) LV_Grid-Link; c) customer plant.*

are calculated while respecting static (e.g. rating of transformer, lines and reactive devices; voltage limits) and dynamic (e.g. reactive power exchange with neighbouring Grid-Links) constraints. The Grid-Link size is variable and depends on the area where the secondary control is set up. In the shown case, secondary control is set up separately within the MVG and the LVG, creating a medium (MV_Grid-Link) and a low voltage Grid-Link (LV_Grid-Link), Figure 1a) and b). Customer plants are considered as black boxes, Figure 1c). Hence, the DSO has neither information nor access to the various appliances within the customer plants.

Figure 1a) shows the MV_Grid-Link. A number of LV_Grid-Links is thereto connected through the BLiNs. The corresponding $VVSC^{MV}$ calculates the var set-points for the neighbouring LV_Grid-Links and the voltage set-point for the MV bus bar of the supplying transformer (STR) while respecting static and dynamic constraints. The LV_Grid-Link is presented in Figure 1b). A number of customer plants is thereto connected through the BLiNs. In this case, the corresponding $VVSC^{LV}$ calculates voltage set-points for the local *L*(*U*)-controls, which are installed to control the voltage in the low voltage Link_Grid. Meanwhile, $VVSC^{LV}$ respects the static constraints and the dynamically changing var constraint at its interface to the MV_Grid-Link. No var set-points are sent to the customer plants. Figure 1c) shows the customer plants. Customers are not requested to contribute to voltage control, thus their PV-inverters inject with a power factor of unity.

## 2.2 *L*(*U*)-control principle

To achieve the maximum effectiveness of the local Volt / var control, the inductive devices are set at the end of the violated feeders [16]. They are equipped with local *L*(*U*)-control. Figure 2 shows a schematic LVG with one *L*(*U*)-controlled feeder, where the inductive device is realized as a shunt coil. The second feeder shown in Figure 2 is too short to violate the

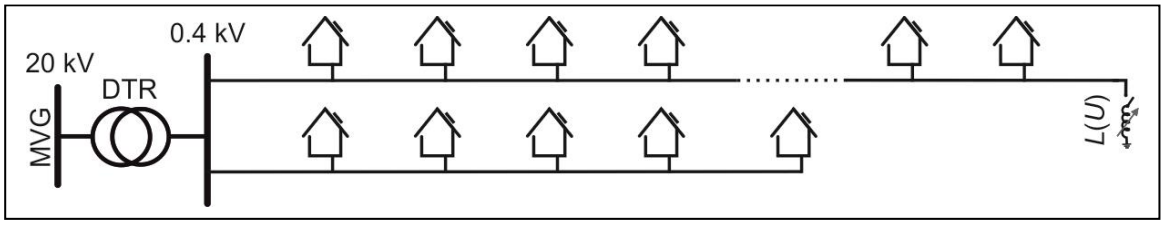


*Figure 2: Schematic LVG with one L(U)-controlled feeder.*

upper voltage limit, thus no inductive device is required to control its voltage. Figure 3 shows the basic *L*(*U*) primary control loop. If the local grid voltage exceeds a voltage set-point

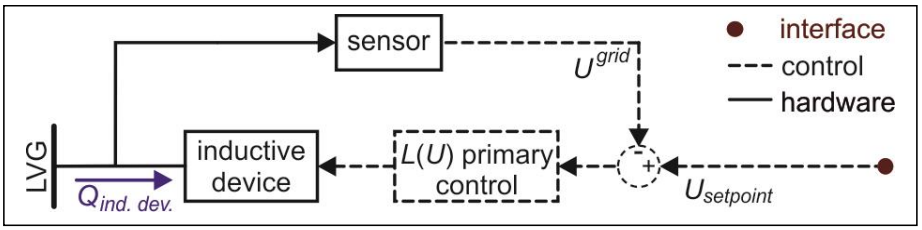


*Figure 3: Basic L(U) primary control loop.*

($U_{setpoint}$), the inductive device is controlled to absorb the reactive power that is needed to keep the grid voltage at $U_{setpoint}$. The voltage set-point can be set onetime when installing the inductive device (local *L*(*U*)-control), or permanently by remote control (coordinated *L*(*U*)-control).

## 3 Comparison of structures between *Q*(*U*)- and *L*(*U*)-control

As preliminary discussed, the coordination of local Volt / var controls on customer plant side entails social and technical issues in the field of cost allocation, data privacy, cyber security and discrimination. Figure 4 shows the structure arising from the coordination of customer-owned PV-inverters. Each customer, who wants to connect a PV-system to the grid, has to

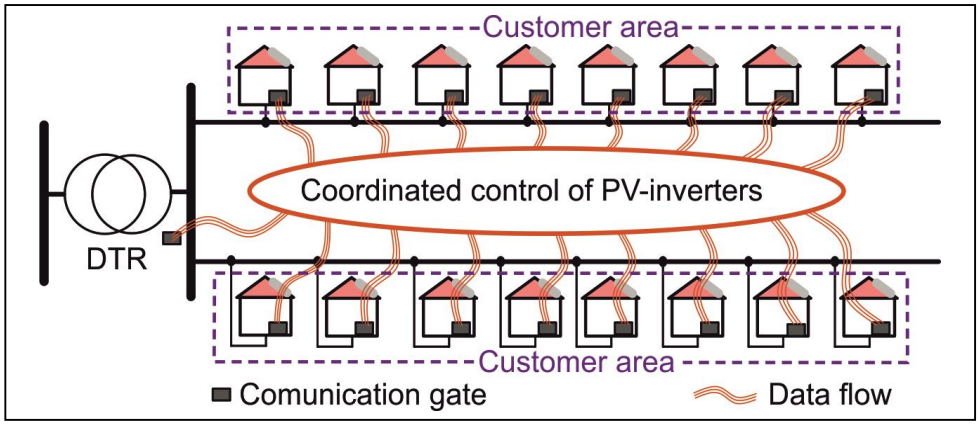


*Figure 4: Structure arising from the coordination of customer-owned PV-inverters.*

invest in controlling units for LVG voltage control. The coordination of these controlling units requires an extensive data flow between the DSO and the involved customers, jeopardizing their data privacy. This data exchange exacerbates the Volt / var management tasks in LVGs and makes the LVG operation vulnerable to cyber-attacks. Studies have shown that the requested reactive power from each customer to achieve a LVG operation within the limits results in a discriminatory ancillary service procurement [17]. The social issues are solved by using DSO-owned inductive devices instead of customer-owned PV-inverters for LVG voltage control. Figure 5 shows the structure arising from the coordination of DSO-owned inductive devices. In this case, the number of needed inductive devices decreases drastically, reducing also the data have to be exchanged for their coordination. DSOs own these devices and have to make the investments for their procurement. The data exchange takes place only between devices owned by the DSO. No data exchange is needed between

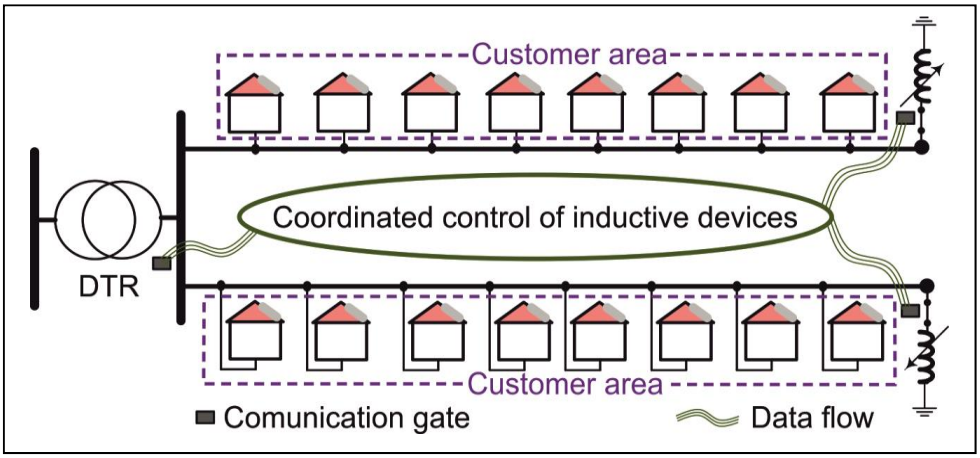


*Figure 5: Structure arising from the coordination of DSO-owned inductive devices.*

the DSO and customers, thus ensuring privacy. Additionally, the reduced data exchange simplifies the LVG's Volt / var management tasks, thus reducing the risk of cyber-attacks. Customers are not obliged anymore to provide ancillary services for the Volt / Var control of LVGs. Hence, the discrimination is impossible in principle.

# 4 Behaviour comparison between *Q*(*U*)- and *L*(*U*)-control

The behaviour of the MVG and LVG in presence of the local *Q*(*U*)- and L(U)-control is analysed by load flow simulations, performed with PSS SINCAL. The used models and the simulated scenarios are described in the following.

## 4.1 Model description

The scope of this study is the behaviour of the MVG and LVG in presence of local Volt / var controls installed in LVGs or customer plants. The simulation model includes a detailed model of a customer plant and a real rural LVG, as well as a simplified model of the MVG.

### 4.1.1 Customer plant model

Figure 6 shows the used structure of each customer plant. It is characterized at each time-point *t* by the active and reactive power consumption and production of the internal loads ($P_{i,t}^{load}$ and $Q_{i,t}^{load}$) and PV-systems ($P_{i,t}^{inv}$ and $Q_{i,t}^{inv}$). Each prosumer *i* is connected to a grid node with a voltage of $U_{i,t}^{grid}$. The load voltage dependency is considered by using a ZIP-model with coefficients for residential loads given in [18]. The *P*- and *Q*-consumption of these loads depends on local grid voltage and is determined by Eqs. (1) and (2). An initial power factor of 0.95 is set for all loads, so that $Q_{init,t}^{load} = P_{init,t}^{load} \cdot \tan(\arccos(0.95))$ . The PV-system of each prosumer contains PV-modules with a rating of $P_r^{PV} = 5$ kW and an inverter with a rating of $S_r^{inv} = P_r^{PV}/0.9$. This over-dimensioning allows to inject with a power factor of 0.9 also during peak active power production. Losses within PV-systems are neglected. The active power consumption and production of loads and PV-systems is determined by Eqs. (3) and (4), respectively, and by the load and PV-production profile shown in Figure 7.

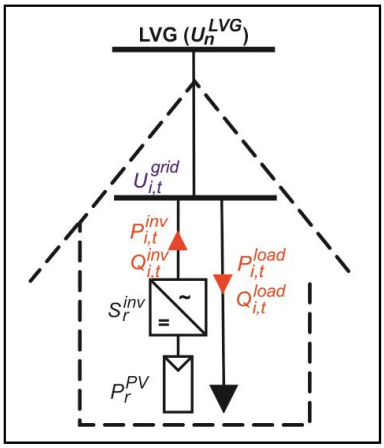


*Figure 6: Structure of each customer plant.*

$$P_{i,t}^{load} = P_{init,t}^{load} \cdot \left( Z_P \cdot \left( u_{i,t}^{grid} \right)^2 + I_P \cdot u_{i,t}^{grid} + P_P \right) \quad (1)$$

$$Q_{i,t}^{load} = Q_{init,t}^{load} \cdot \left( Z_Q \cdot \left( u_{i,t}^{grid} \right)^2 + I_Q \cdot u_{i,t}^{grid} + P_Q \right) \quad (2)$$

where:

$u_{i,t}^{grid} = \frac{U_{i,t}^{grid}}{U_n^{LVG}}$ … normalized grid voltage at prosumer *i* for time-point *t*

$Z_P, I_P, P_P$ … active power ZIP-coefficients

$Z_Q, I_Q, P_Q$ … reactive power ZIP-coefficients

In Figure 7 is also marked a critical time-point ($t_{crit}$), where the PV-production is maximal.

$P_{init,t}^{load} = f_t^{load} \cdot \hat{P}^{load}$ , where $\hat{P}^{load} = 1.37$ kW (3)

$P_{i,t}^{inv} = f_t^{PV} \cdot P_r^{PV}$ (4)

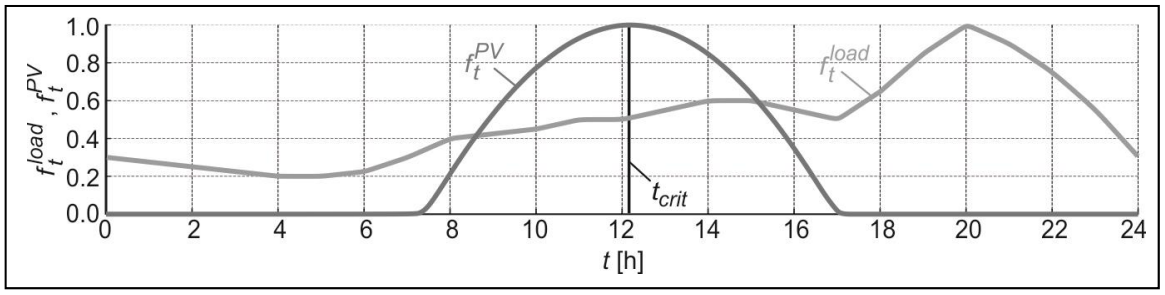


*Figure 7: Load and PV-production profile of all prosumers connected to the rural LVG.*

Meanwhile, the reactive power consumption or production of each PV-inverter is determined by the applied control strategy. In this study, we focus on the grid behaviour in presence of local Volt / var controls. Three cases are considered: no-control, local *Q*(*U*)- and local *L*(*U*)-control.

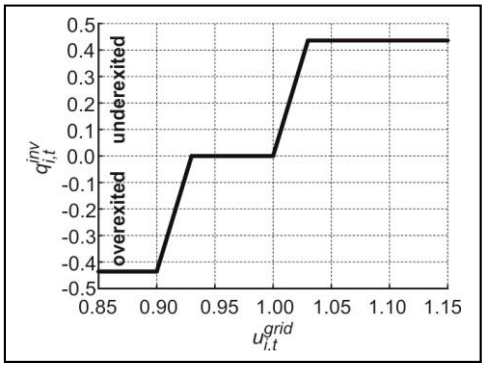


*Figure 8: Simulated Q(U)-characteristic.*

**No-control** – In this case, voltage in LVG is not controlled. Hence, no local *L*(*U*)-controls are installed and PV-inverters of customer inject with a power factor of unity.

**Local *Q*(*U*)-control** – A *Q*(*U*)-controlled PV-inverter injects reactive power depending on the local grid voltage. Figure 8 shows the simulated *Q*(*U*)-characteristic, which is identified to be appropriate for the considered rural LVG in Ref. [13]. On the ordinate is plotted the normalized reactive power contribution of the inverter: $q_{i,t}^{inv} = \frac{Q_{i,t}^{inv}}{S_r^{inv}}$.

**Local *L*(*U*)-control** – If local *L*(*U*)-control is applied, inductive devices with continuous variable reactances are set at the end of each violated feeder. The exact positions of the inductive devices within the LVG model are marked in Figure 9. The voltage set-point is set to $U_{setpoint}$ = 1.09 pu and active power losses of inductive devices are neglected.

### 4.1.2 Low voltage grid model

Figure 9 shows a schematic presentation of the rural LVG. It is a real grid with four main feeders. The longest of them is 1.63 km, while the shortest is 0.565 km long. In this grid with

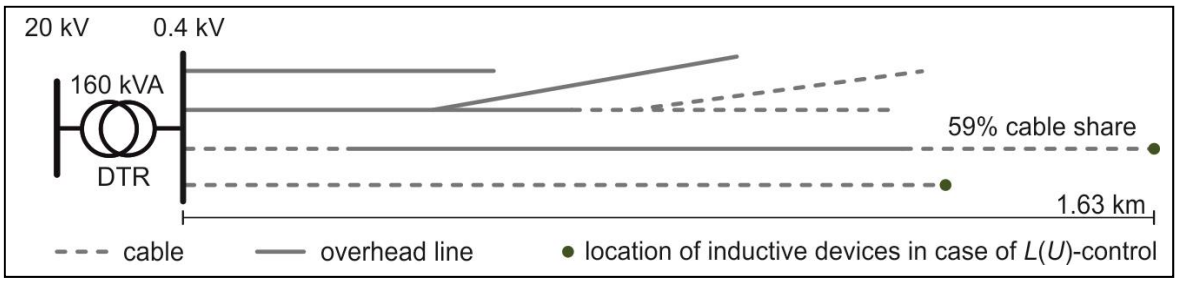


*Figure 9: Schematic presentation of the rural low voltage grid.*

a 59% cable share are connected 61 customer plants. It is connected to the MVG through a 20 kV / 0.4 kV, 160 kVA DTR. The DTR has a fixed tap set in middle position. The complete data of the considered LVG model is given in [19].

### 4.1.3 Medium voltage grid model

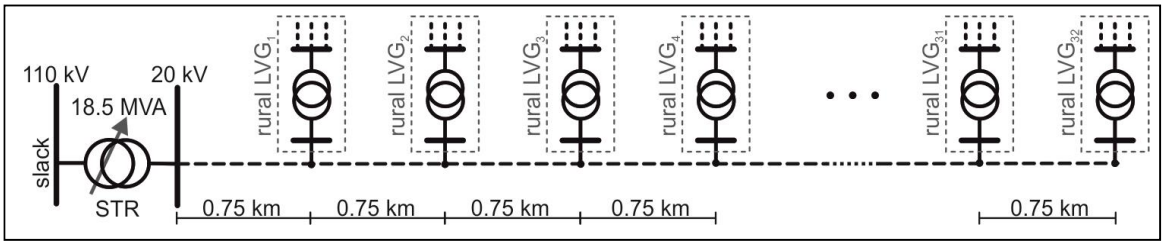


*Figure 10: Schematic presentation of the theoretical medium voltage grid.*

Figure 10 shows a theoretical MVG with one 24 km long main feeder. In this grid with a 100% cable share are equidistantly connected 32 rural LVGs described in section 4.1.2. It is connected to the slack node through a 110 kV / 20 kV, 18.5 MVA supplying transformer (STR). The STR has an On-Load tap Changer (OLTC) with 25 tap positions and a voltage step of 1.667%. The OLTC is locally controlled to keep the voltage at the 20 kV side between 0.98 and 1.02 pu. The medium voltage cable has a specific resistance, reactance and capacitance of 0.206 Ω/km, 0.122 Ω/km and 254 nF/km, respectively.

## 4.2 Scenario definition

Two different grid models are simulated: Firstly, only the LVG with connected customer plants is considered and the slack node is located at the primary side of the DTR. Secondly, both grid-types (MVG and LVGs) and the customer plants are considered. In this case, the slack node is located at the primary side of the STR.

No-control, local *Q*(*U*)-control, and local *L*(*U*)-control are separately simulated in both grid models.

### 4.2.1 Low voltage grid simulations

The load and PV-production profile shown in Figure 7 is sampled into one minute time-steps, resulting in 1440 load flow simulations per scenario. The slack voltage is set to 1.01 pu.

### 4.2.2 Combined medium and low voltage grid simulations

In this case, only the critical time-point ($t_{crit}$) marked in Figure 7 is simulated. The slack voltage is set to 1.02 pu.

## 4.3 Simulation results

This section presents the simulation results for no-control, local $Q(U)$-control and local $L(U)$-control. The grid behaviour is evaluated by four parameters: the reactive power exchange at DTR primary side ($Q^{ex}$), the active power loss ($P^{loss}$) including DTR and line losses, the DTR loading, and the voltage profiles of all LVG feeders. For the combined medium and low voltage grid simulations are shown the voltage profiles of the MVG and of all feeders of selected LVGs.

### 4.3.1 Low voltage grid simulations

Figure 11 shows the daily behaviour of $Q^{ex}$, $P^{loss,}$ and the DTR loading for no-control and both control strategies. Their maximum values appear at about $t_{crit}$ in all cases. $Q(U)$-control provokes the maximum values, while no-control provokes the minimum ones. Figure 11a)

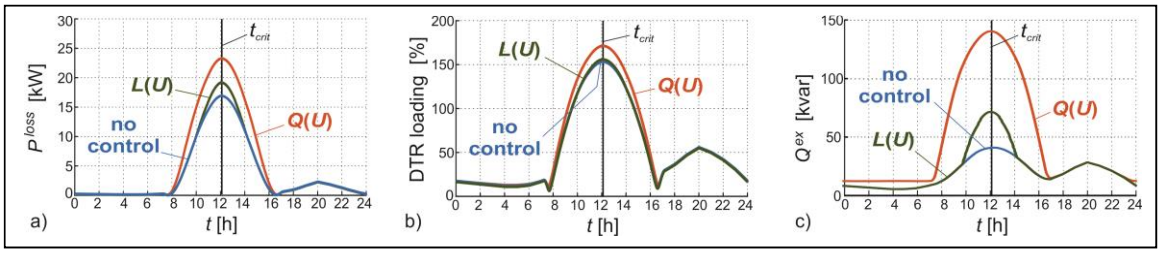


*Figure 11: Daily behaviour of the secondary criteria for no-control and different control strategies: a) losses; b)* DTR loading*; c) Q-exchange.*

shows the active power loss. The maximum values are about 16.89 kW, 23.27 kW and 19.29 kW for no-, $Q(U)$- and $L(U)$-control, respectively. The DTR loading is presented in Figure 11b). The maximum values reach about 153 %, 171 % and 156 % for no-, $Q(U)$- and $L(U)$-control, respectively. Figure 11c) shows the reactive power exchanged at the DTR primary side. A maximum $Q$-exchange of approximately 41 kvar, 141 kvar and 72 kvar appears for no-, $Q(U)$- and $L(U)$-control, respectively. For no-control, $Q^{ex}$ refers to the loads', lines' and DTR's reactive power consumption, thus following mainly the load profile shown in Figure 7. For both control strategies, the total reactive power consumption of all control devices, i.e. PV-inverters in case of $Q(U)$-control and inductive devices in case of $L(U)$-control, accrues to the reactive power exchange.

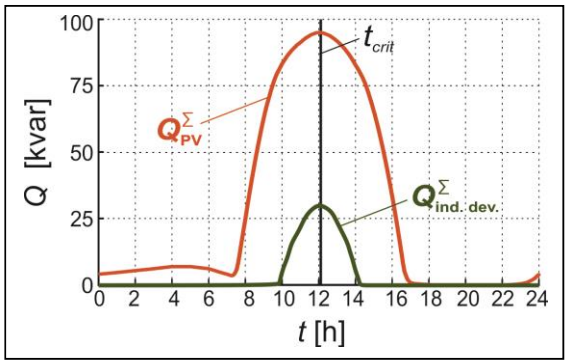


*Figure 12: Total reactive power consumption of all control devices in case of Q(U)- and L(U)-control.*

Figure 12 shows the total reactive power consumption of all control devices for both control strategies. They reach their maximum *Q*-consumption of 95 kvar and 30 kvar for *Q*(*U*)- and *L*(*U*)-control, respectively, at about $t_{crit}$.

Figure 13 shows the voltage profiles of all feeders of the rural LVG for no-control and different control strategies at $t_{crit}$. Figure 13a) shows them for no-control. The upper voltage limit is violated by one feeder. A maximum voltage of about 1.12 pu is reached at its end. In Figure 13b) are presented the voltage profiles for *Q*(*U*)-control. In this case, the voltages are decreased more than necessary to alleviate the violation of the upper voltage limit, resulting in a maximum voltage of about 1.075 pu. The profiles for *L*(*U*)-control are shown in Figure 13c). Here, the limit violations are eliminated and a voltage of 1.09 pu is reached at the feeder end.

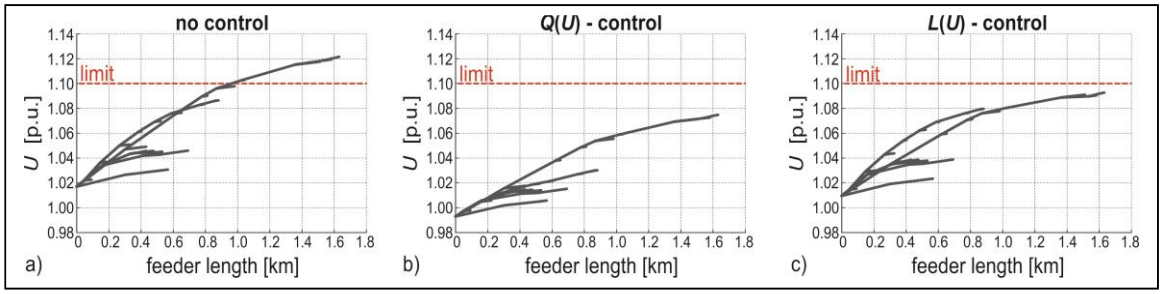


*Figure 13: Voltage profiles of all feeders of the rural LVG at $t_{crit}$ for no-control and different control strategies: a) no-control; b) local Q(U)-control; c) local L(U)-control.*

### 4.3.2 Combined medium and low voltage grid simulations

Figure 14 shows the voltage profiles of the MVG feeder and all feeders of selected rural LVGs for no-control and both control strategies at $t_{crit}$. In all three cases, the OLTC stayed in its middle position. For no-control, violations of the upper voltage limit appear in all LVGs. The upper voltage limit in MVG is not violated. MVG. If *Q*(*U*)-control is applied, all limit violations are alleviated, and the voltages in MVG are drastically decreased. It can be seen, that the voltage drop over the DTRs is very large in this case. Using local *L*(*U*) to control LVG voltages also alleviates all limit violations, but has a smaller effect on MVG voltages compared to the previously discussed case; also the voltage drop over the DTRs is much smaller.

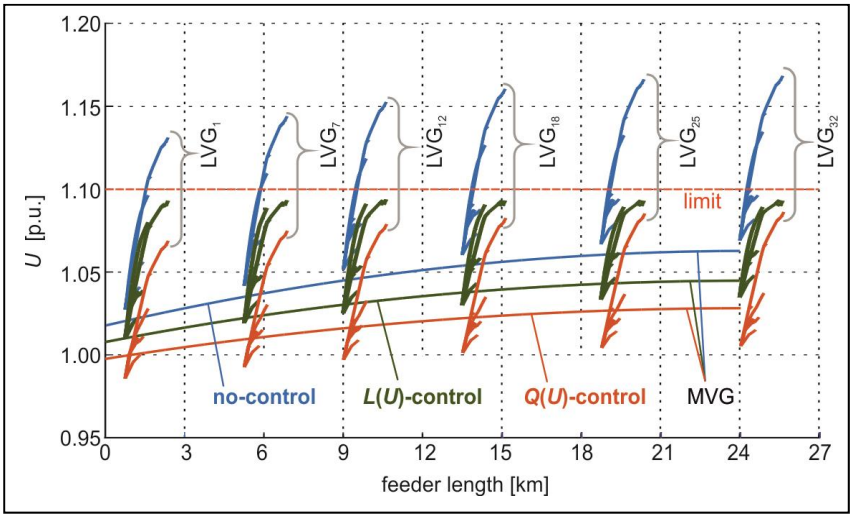


*Figure 14: Voltage profiles of the MVG feeder and all feeders of selected rural LVGs at $t_{crit}$ for different control strategies.*

# 5 Conclusion

In LVGs with high rooftop PV penetration, the proposed *L*(*U*)-control installed at the end of violated feeders eliminates the violation of upper voltage limit. DSOs own and operate the *L*(*U*)-control units. Thus, the investment to control the voltage in LVG are shifted from customers (*Q*(*U*)-control) to DSOs (*L*(*U*)-control). The discrimination of the customers on reactive power delivery disappears, because they are not requested to provide such an ancillary service. No data exchange between the DSO and the customers is necessary to coordinate the local Volt / var controls. Therefore, their data privacy is guaranteed. The number of data needed for the coordination of the local *L*(*U*)-controls is very small thus reducing the threat to cyber-attacks. Besides, their Volt / var management is simplified. Additionally, simulation results show that the local *L*(*U*)-control has substantial technical advantages compared to the local *Q*(*U*)-control. If *L*(*U*)-control is applied then grid losses, distribution transformer loading and the uncontrolled reactive power flow between medium- and low-voltage grid are smaller than in the *Q*(*U*)-control case. The effect on the voltages of the superordinate medium-voltage grid is reduced.

**References**

[1] S. Hashemi and J. Østergaard, "Methods and strategies for overvoltage prevention in low voltage distribution systems with PV," in *IET Renewable Power Generation*, vol. 11, no. 2, pp. 205-214, 2017, doi: 10.1049/iet-rpg.2016.0277.

[2] M. H. J. Bollen and A. Sannino, "Voltage control with inverter-based distributed generation," in *IEEE Transactions on Power Delivery*, vol. 20, no. 1, pp. 519-520, 2005, doi: 10.1109/TPWRD.2004.834679.

[3] International Energy Agency, “World Energy Outlook 2018“, 2018, ISBN: 978-92-64-30677-6.

[4] E. Demirok, P.C. González, K.H.B. Frederiksen, D. Sera, P. Rodriguez, R. Teodorescu, “Local reactive power control methods for overvoltage prevention of distributed solar inverters in low-voltage grids,” in *IEEE J. Photovolt.*, vol. 1(2), pp. 174-182, 2011, doi: 10.1109/JPHOTOV.2011.2174821.

[5] R. Caldon, M. Coppo, R. Turri, “Distributed voltage control strategy for LV networks with inverter-interfaced generators,” in *Elsevier EPSR*, vol. 107, pp. 85-92, 2014, doi: 10.1016/j.epsr.2013.09.009.

[6] B. Bletterie, S. Kadam, R. Bolgaryn and A. Zegers, "Voltage Control with PV Inverters in Low Voltage Networks—In Depth Analysis of Different Concepts and Parameterization Criteria," in *IEEE Transactions on Power Systems*, vol. 32(1), pp. 177-185, 2017, doi: 10.1109/TPWRS.2016.2554099.

[7] J. Hrouda, F. Kysnar, K. Prochazka and K. Hojdar, "Implementation of Q/U function of photovoltaic power plants in low voltage distribution networks," in *17th International Scientific Conference on Electric Power Engineering (EPE)*, Prague, 2016, pp. 1-6. doi: 10.1109/EPE.2016.7521820.

[8] Proposal for a DIRECTIVE OF THE EUROPEAN PARLIAMENT AND OF THE COUNCIL on common rules for the internal market in electricity (recast), COM/2016/0864 final - 2016/0380 (COD).

[9] A. Ilo, “Effects of the Reactive Power Injection on the Grid - The Rise of the Volt/var Interaction Chain,” in *Smart Grid and Renewable Energy*, vol. 7, pp. 217-232, 2016, doi: 10.4236/sgre.2016.77017.

[10] N. Karthikeyan, B. R. Pokhrel, J. R. Pillai and B. Bak-Jensen, "Coordinated voltage control of distributed PV inverters for voltage regulation in low voltage distribution networks," *2017 IEEE PES Innovative Smart Grid Technologies Conference Europe (ISGT-Europe)*, Torino, 2017, pp. 1-6, doi: 10.1109/ISGTEurope.2017.8260279.

[11] M. Juamperez, G. Yang, S.B. Kjaer, “Voltage regulation in LV grids by coordinated volt-var control strategies,” in *J. Mod. Power Syst. Clean Energy*, 2014, doi: 10.1007/s40565-014-0072-0.

[12] A. Cagnano, E. De T uglie, M. Bronzini, ”Multiarea Voltage Controller for Active Distribution Networks,” in *Energies*, vol. 11, 583, 2018, doi: 10.3390/en11030583.

[13] D.-L. Schultis, A. Ilo, C. Schirmer, “Overall performance evaluation of reactive power control strategies in low voltage grids with high prosumer share,” in *Elsevier Electric Power Systems Research*, vol. 168, pp. 336-349, 2019, doi: 10.1016/j.epsr.2018.12.015.

[14] A. Ilo, “Link - The smart grid paradigm for a secure decentralized operation architecture,” in *Elsevier Electric Power Systems Research*, vol. 131, pp. 116-125, 2016, doi: 10.1016/j.epsr.2015.10.001.

[15] A. Ilo, D.-L. Schultis, “Low-voltage grid behaviour in the presence of concentrated var-sinks and var-compensated customers,” in *Elsevier Electric Power Systems Research* (in press).

[16] A. Ilo, D.-L. Schultis, C. Schirmer, “Effectiveness of Distributed vs. Concentrated Volt/Var Local Control Strategies in Low-Voltage Grids,” in *Applied Sciences*, vol. 8(8), 1382, 2018, doi: 10.3390/app8081382.

[17] M. A. Azzouz and E. F. El-Saadany, "Optimal coordinated volt/var control in active distribution networks," in *2014 IEEE PES General Meeting | Conference & Exposition*, National Harbor, MD, pp. 1-5, 2014, doi: 10.1109/PESGM.2014.6939137.

[18] A. Bokhari *et al*., "Experimental Determination of the ZIP Coefficients for Modern Residential, Commercial, and Industrial Loads," in *IEEE Transactions on Power Delivery*, vol. 29(3), pp. 1372-1381, 2014, doi: 10.1109/TPWRD.2013.2285096.

[19] D.-L. Schultis, A. Ilo, “TUWien_LV_TestGrids,” in *Mendeley*, v1, 2018, doi: 10.17632/hgh8c99tnx.1 (dataset).